

Domain-wall dynamics of magnetic systems with disorder at zero temperature

N. J. Zhou¹, B. Zheng^{1*} and Y.Y. He¹

¹ *Zhejiang University, Zhejiang Institute of Modern Physics, Hangzhou 310027, P.R. China*

Abstract

With Monte Carlo simulations, we investigate the relaxation dynamics with a domain interface in a magnetic system at zero temperature, taking two-dimensional driven random field Ising model with quenched disorder as an example. The dynamic scaling behavior is carefully analyzed, and a dynamic roughening process is observed at the depinning transition. For comparison, additional simulation without disorder has been performed as its background. The effect of the overhangs is discussed, and the growing interface exhibits intrinsic anomalous scaling and spatial multiscaling with $\zeta > 1$ and $\zeta_{loc} < 1$, different from the work described by QEW.

PACS numbers: 64.60.Ht, 68.35.Rh, 05.10.Ln

* corresponding author: zheng@zimp.zju.edu.cn

I. INTRODUCTION

In the past years much progress has been achieved in the study of dynamic processes far from equilibrium. For example, the universal dynamic scaling form in critical dynamics has been explored up to the *macroscopic* short-time regime [1–4], when the system is still far from equilibrium. Although the spatial correlation length is still short in the beginning of the time evolution, the dynamic scaling form is induced by the divergent correlating time around a continuous phase transition. Based on the short-time dynamic scaling form, new methods for the determination of both dynamic and static critical exponents as well as the critical temperature have been developed [2–5]. Since the measurements are carried out in the short-time regime, one does not suffer from critical slowing down. Recent progress in the short-time critical dynamics includes, for example, theoretical calculations and numerical simulations of the XY models and Josephson junction arrays [6], magnets with quenched disorder [7–10], ageing phenomena [11], weak first-order phase transitions [8, 12], and various applications and developments [13].

Meanwhile, the physics of elastic systems in disordered media also has been the focus of intense theoretical and experimental studies in the different areas, such as charge density waves [14], vortex lattices [15], domain walls in magnetic [16, 17] or ferroelectric [18, 19] materials, contact lines [20, 21], fluid invasion of porous media [22], dislocations moving [23, 24], and crack propagation [25]. With increasing driving force F , the driven interface in quenched disordered system displays a transition from a pinned interface to a moving interface. This so-called pinning-depinning phase transition at zero temperature is viewed as a critical phenomenon [26–35], and its ordered parameter is the interface velocity v . With the assumption that the interface shows the properties of an elastic membrane, this growth process can be described by the driven Edwards-Wilkinson equation with quenched disorder (QEW) in the isotropic universality class [32–38] or the driven quenched Kardar-Parisi-Zhang equation (QKPZ) [39–42] in the anisotropic universality class. With these equations, all the critical exponents can be derived by simulation and theory analysis called functional renormalization group (FRG) [29, 36, 43]. And the roughness exponent $\zeta > 1$ obtained from the equation QEW in $1 + 1$ dimensions means that the elastic string will inevitably break as the length of the string is increased [34, 37, 38, 40].

Recently, these kinetic roughening phenomenons have brought about interest on the su-

perrough growth of the interface or surface with $\zeta > 1$, not only in simulations [44–46], but also in experiment [47–49]. Three scaling behaviors have been observed experimentally, namely, (i) FV standard scaling for $\zeta = \zeta_{loc} = \zeta_s < 1$; (ii) intrinsic anomalous scaling for $\zeta \neq \zeta_{loc} = \zeta_s \leq 1$; and (iii) superrough scaling for $\zeta = \zeta_s > \zeta_{loc} = 1$. Here roughness exponent ζ , local roughness exponent ζ_{loc} and spectral roughness exponent ζ_s can be measured in different ways, such as globe width function $W(L, t)$, local width function $W(l, t)$, height correlation function $C(r, t)$, local interfacial orientation $W_n(l, t)$, and power spectral density $S(k, t)$. And spatial multiscaling behavior is observed associated with the intrinsic anomalous scaling class (ii) [44, 45, 47].

On the other hand, many recent activities have been devoted to the domain-wall dynamics in the magnetic materials, which is an important topic in magnetic devices, nano-materials, thin film, and semiconductors [16, 17, 50–54]. And external field H or electrical current J is applied as the driving force F . At zero temperature, the depinning transition is obtain when the homogeneous driving field H reaches its critical value H_c , which is relation with the disorder. And if a periodic external field $H(t) = H_0 \cos(\omega t)$ is applied and/or a non-zero temperature is introduced, the domain wall exhibits different states of motion and dynamic phase transitions [52, 53, 55, 56]. Most these works concentrate on the stationary state at the zero or low temperatures and in response to the external magnetic field $H(t)$. Instead of the phenomenological model, such as QEW or QKPZ equation, a well established model to investigate the dynamics behavior of the domain interface is the driven random field Ising model (RFIM) [26–28, 57–59]. The scaling behavior and critical exponents have been obtained for various dimensions at zero or low temperature, which is roughly consistent with the result of QEW. While as we well known, the roughness growth is rarely to be investigated because lots of overhangs occur at the depinning transition and it is hard to determine the critical exponents and transition point precisely by the finite-size scaling and finite-temperature scaling analysis in the stead state

Very recently, the experiment on the non-stationary dynamic evolution of the domain wall is reported for the creep and pinning effect [60], though its dynamic behavior is described roughly. What’s more, the short-time relaxation of a driven elastic string in a two-dimensional pinning landscape is also reported in the reference [33], in order to get the critical exponents of the depinning transition independently. Additional, the short time dynamic relaxation of a domain wall has been concerned for magnetic systems at a stan-

dard order-disorder phase transition in the Ising model [9, 10, 13]. It is described by the relaxation dynamics starting from a *semi-ordered* state, and shares certain common features with those around free and disordered surfaces. Since no external magnetic fields are added, macroscopically the domain wall does not move, but a kind of roughening phenomena occurs.

In this paper, we investigate the relaxation dynamics of domain walls at zero temperature for the depinning transition, taking the two-dimensions driven RFIM as an example. And we aim at understanding the non-stationary properties of this dynamics system and determining the static and dynamic exponents as well as the transition point. Then the effect of overhangs will be studied by the roughness scaling behavior, which causes the main difference between QEW and RFIM at the depinning transition. For comparison, its background in our work is also investigated without overhangs. In Sec. II, the model and scaling analysis are described, and in Sec. III, the numerical results are presented. Sec. IV includes the conclusions.

II. MODEL AND SCALE ANALYSIS

The random-field Ising model is defined by the Hamiltonian

$$\mathcal{H} = -J \sum_{\langle ij \rangle} S_i S_j - H \sum_i S_i - \sum_i h_i S_i. \quad (1)$$

Where $S_i = \pm 1$ is just the Ising spin on the two-dimensional lattice with $L \times L$. The random field h_i is taken from a distribution within an interval $[-\Delta, \Delta]$ and hence is bounded. H is the homogeneous driving field. The strength of the random field is fixed as $\Delta = 1.5J$ in this paper, and $\Delta = 0J$ is also used in comparison as its background. For convenience, we set $J = 1$ in this paper. The main simulation is performed with the lattice of size $L = 512$ at zero temperature, and the maximum updating time is $t_M = 1024$. Additional simulation with $L = 256$ and $L = 1024$ are also performed to exclude the finite-size effect. The total samples for average are 50000, and the statistical error are estimated by dividing the samples into two or three groups. If the fluctuation in the time direction is comparable with or larger than the statistical error, it will be taken into account.

The initial semi-ordered state is such a state that spins are positive in the sublattice on the left side $x < 20$ and negative on the right side $x > 20$. Here we set the x axis in the direction perpendicular the initial interface and its left boundary is located at $x = 0$. Then all the system is rotated by an angle $\pi/4$ in order to make sure that the initially interface

of the system is just in the (11)-direction of the lattice. Therefore there is no pinning of the interface without the disorder [26–28]. The antiperiodic conditions are used in the x direction. While in the other direction, periodic conditions are used. After preparing that, we perform Monte Carlo simulations and the spins are chosen randomly to update. And the spins will be flipped only when the total energy decreases after flipped. As time evolves, the interface moves due to the driving field and becomes more and more roughening. In Fig. 1(a), the real snapshot images of this interface are illustrated in the dynamic relaxation process for the depinning transition and its background. The local interface at the transition point not only tilts, but also forms local grooves or spikes, quite different from the instance of the background. Hence, it is difficult to define the height function $h(t)$ of the interface because of visible overhangs.

In this case, we define the velocity of the domain interface as the time derivation of the magnetization[28]. First, the magnetization and its second moment are measured,

$$M^{(k)}(t) = \frac{1}{L^{2k}} \left\langle \left[\sum_{x,y=1}^L S_{xy}(t) \right]^k \right\rangle, \quad k = 1, 2. \quad (2)$$

Here $S_{xy}(t)$ is a spin at the time t on the lattice position (x, y) , and $\langle \dots \rangle$ represents the statistical average over disorder. For convenience, we also use $M(t) \equiv M^{(1)}(t)$ to denote the magnetization. Then the velocity of the domain interface is shown,

$$v(t) = \frac{L}{2} \frac{d M(t)}{d t}. \quad (3)$$

Here $L/2$ is the scale factor. In order to characterize the growth of the domain interface and its fluctuation in the x direction, we introduce a height function and its second moment

$$h^{(k)}(t) = \frac{1}{L^k} \left\langle \left[\sum_{x=1}^L S_{xy}(t) \right]^k \right\rangle, \quad k = 1, 2. \quad (4)$$

Here $\langle \dots \rangle$ represents not only the statistic average but also the average in the y direction. As usual, we also use the notation $h(t) \equiv h^{(1)}(t)$ and the relation $h(t) \equiv M(t)$ is obtained. Then the roughness function of the domain interface is defined,

$$\omega^2(t) = h^{(2)}(t) - h(t)h(t). \quad (5)$$

After that, the relation between the magnetization fluctuation and interface fluctuation can be described in the function $F(t)$,

$$F(t) = \frac{M^{(2)}(t) - M(t)M(t)}{h^{(2)}(t) - h(t)h(t)}. \quad (6)$$

What's more, a more informative quantities for the interface, called the height correlation function $C(r, t)$, is introduced.

$$C(r, t) = \langle [h(y + r, t) - h(y, t)]^2 \rangle. \quad (7)$$

Here $h(y, t)$ describes the local interface height and can be obtained by Eq. (4) with a fixed y .

At the depinning transition point $H = H_c(\Delta)$, the main scale length in the dynamic system is the non-equilibrium spatial correlation length $\xi(t)$. For a finite size, the lattice size L is an additional length scale. And the system exhibits as the second-order transition when temperature is zero. So one can believe that $\xi(t)$ grows as a power law $\xi(t) \sim t^{1/z}$ and z is so-called dynamic exponent. General scaling arguments lead to the scaling form of the order parameter $v(t)$.

$$v(t) = (\xi(t))^{-\beta/\nu} G(\xi(t)/L, \tau/\xi(t)). \quad (8)$$

Here β and ν are the static exponents and $\tau = H - H_c$ is defined as the departure from the transition point. And the scaling function $G(\xi(t)/L, \tau/\xi(t))$ is constant if $L \rightarrow \infty$ and $\tau = 0$. Then the scaling form is simplified to

$$v(t) \sim t^{-\beta/\nu z}. \quad (9)$$

And the scaling behavior of the derivative $\partial_\tau \ln v(t, \tau)|_{\tau=0}$ can be obtained according to Eq. (8).

$$\partial_\tau \ln v(t, \tau)|_{\tau=0} \sim t^{1/\nu z}. \quad (10)$$

In general, the height function $h(t)$, the roughness function $\omega^2(t)$ and the height correlation function $C(r, t)$ in Eqs. (4), (5) and (7) do not obey a simple power law behaviors. Since the depinning transition is a dynamic transition and its order parameter is $v(t) \sim dh(t)/dt$. And in the background without disorder, the interface is also roughening. So pure roughness function and height correlation function should be defined by subtracting the contribution from the background.

$$D\omega^2(t) = \omega^2(t) - \omega_b^2(t). \quad (11)$$

$$DC(r, t) = C(r, t) - C_b(r, t). \quad (12)$$

And the scaling form of $D\omega^2(t)$ and $DC(r, t)$ are shown as in the case of a standard growing interface, reported in Refs. [30, 31, 44].

$$D\omega^2(t) \sim t^{-2\zeta/z}. \quad (13)$$

$$DC(r, t) \sim \begin{cases} \xi(t)^{2(\zeta - \zeta_{loc})} r^{2\zeta_{loc}} & \text{if } r \ll \xi(t) \\ \xi(t)^{2\zeta} & \text{if } \xi(t) \ll r \end{cases}. \quad (14)$$

Here $\xi(t) \sim t^{1/z}$ and z have been defined before. And ζ is the roughness exponent and ζ_{loc} is the local one. Since the region with the power law behavior for $DC(r, t)$ vs. r is rather narrow, a new scaling form is introduced to fit this relation [30, 31].

$$DC(r, \infty) = A[\tanh(r/B)]^{2\zeta_{loc}}. \quad (15)$$

Then, the roughness function $\omega^2(t)$ represents the fluctuation only in the x direction, while the fluctuation of the magnetization is measured in the whole lattice. So the scaling behavior of the function $F(t)$ is shown,

$$F(t) = \xi(t)^{d-1} \sim t^{1/z}. \quad (16)$$

What's more, all the scaling behaviors above hold only after a time scale t_{mic} , which is sufficiently long in the microscopic sense, but still short in the macroscopic sense. Hence, a power law correction to the scaling is used sometimes in order to fit the data well.

$$Y(x) \sim x^a(1 + c/x). \quad (17)$$

Here the convergence of $Y(t)$ is to a power law behavior and the parameter a is viewed as the critical exponent.

III. THE RESULT OF NUMERICAL SIMULATION

Firstly, the depinning transition of the 2D driven RFIM is measured carefully by the short time dynamics in Fig. 1(b) with different driving field H and the disorder is fixed as $\Delta = 1.5$. The transition point $H_c = 1.2933(2)$ is obtained according to general scaling theory, which is more precise than $H_c = 1.290(5)$ obtained through the steady state near the depinning transition [28]. Then the exponent $\beta/\nu z = 0.217(2)$ is measured from the slope of the curve at the transition point, according to Eq. (9). And the finite size effect is also checked with the different lattice size $L = 256$ and 1024 . Then in Fig. 2(a), the fluctuation function $F(t)$, defined in Eq. (6), is plotted for the depinning transition and its background, respectively. And basing on Eq. (16), the exponent $1/z = 0.749(5)$ and $1/z_b = 0.677(3)$ are derived from the slopes of the dash lines. Here z is the dynamic exponent for the depinning

transition with $\Delta = 1.5$, $H_c = 1.2933$ and z_b is for the background with $\Delta = 0$, $H_c = 1.2933$. Then the time evolution of the derivative $\partial_\tau \ln v(t, \tau)|_{\tau=0}$ is displayed in Fig. 2(b) with open circles and its slope 0.729(4) is measured. In order to fit the numerical data well, a power law correlation is introduced, according to Eq. (17). With Eq. (10), $1/\nu z = 0.735(3)$ can be measured. Following, in Fig. ??(a), the roughness function $\omega^2(t)$ is plotted with open dots and their slopes are 1.701(6) for the depinning transition and 0.666(4) for the background. Then the pure roughness function $D\omega^2(t)$, defined in Eq. (11), is shown with pluses and the exponent $2\zeta/z = 1.717(5)$ is obtained according to Eq. (13), using this power law correction form again. In the same way, the exponent $2\zeta_b/z_b = 0.649(4)$ is also derived. Here ζ and ζ_b denote the roughness exponent for the depinning transition and the background, respectively.

Combing the exponents $\beta/\nu z, 1/\nu z, 1/z$ and $2\zeta/z$, one can calculate these critical exponents $\beta = 0.295(2)$, $\nu = 1.02(1)$, $z = 1.33(1)$ and $\zeta = 1.14(1)$ independent for the depinning transition. Then for its background, $z_b = 1.50(1)$ and $\zeta_b = 0.487(5)$ are obtained. Finally, in Fig. ??(b), the curves about the pure height correlation function $DC(r, t)$ are plotted with open dots. For a sufficiently large scale $r \gg \xi(t)$, e.g., $r = 256$, the exponent $2\zeta/z = 1.701(7)$, derived with the scaling analysis in Eq. (14), is well consistent with 1.717(5) obtained in Fig. ??(a). What's more, for a sufficiently small scale $r \ll \xi(t)$, e.g., $r = 2$, the curve also obeys a power law behavior and the exponent $2(\zeta - \zeta_{loc})/z = 0.597(4)$ is also obtained. With $z = 1.33(1)$ at hand, one can calculate that $2\zeta_{loc} = (1.701 - 0.597) \times 1.33 = 1.47$. Then in the inset, the height correlation function $DC(r, \infty)$ vs. r is plotted for the depinning transition at the sufficiently larger time, e.g., $t = 1024$. And a special scaling form in Eq. (15) is used to fit the data in the whole regime and $2\zeta_{loc} = 1.46(3)$ is measured for the depinning transition, which is also well consistent with the exponent $2\zeta_{loc} = 1.47$ obtained before.

Finally, the critical exponents characterizing the velocity of the domain interface, the roughness function and the height correlation function are extracted, and all the results are summarized in the last column of Table I. For comparison, some exponents, obtained by the driven QEW equation, the driven RFIM in the steady state, the discrete dislocation dynamics at the depinning transition and the forced-flow imbibition in columnar geometries, are also listed here. As was mentioned in the introduction, there are arguments in favor of the conjecture that the motion of a domain wall in a random-field system can be described by the driven QEW equation with quenched disorder [57]. While our findings doesn't support this

conjecture, because there are at least 10% difference between these two models. Hence, they are in the different universality classes. While the theory values of these exponents for QEW have been derived by the function renormalization group(FRG) with $z = 1.33, \zeta = 1.00$ for the one-loop order and $\beta = 0.31, \nu = 0.98, \zeta = 1.43$ for the two-loop order [29]. With this, one can see that some critical exponents in our work is well consistent with the theory value. Then these two measurements of the roughness exponent ζ by the pure roughness function $D\omega^2(t)$ and the pure height correlation function $DC(r, t)$ are in good agreement. And $\zeta = 1.13(1) > 1$ and $\zeta_{loc} = 0.743(6) < 1$ mean that the interface growth process with intrinsic anomalous scaling and spatial multiscaling takes place. It is quite different with the interface growth process with superrough scaling and spatial single scaling in QEW with $\zeta = 1.23 > 1$ and $\zeta_{loc} = 0.98 \approx 1$. The dynamic equation QEW is used to describe a one-dimensional driven elastic string in a two-dimensional disordered medium. Then the position of the interface can be defined uniquely and there are practically no overhangs, bubbles or droplets. So the single spatial scaling behavior is easy to understand. While overhangs is obvious in our work of RFIM, shown in Fig. 1(a). Hence, we guess it is overhangs cause this spatial multiscaling behavior, which is rarely in QEW. And additional simulation for the background in our work also supports this hypothesis. In our work, we confirm that the one-order transition takes place at $H_c = \Delta$, for the pinning-depinning process with $\Delta \leq 1$ [26]. Hence, in our simulation of the background without disorder, a steady velocity state is obtained with the large driving field $H \gg H_c = 0$. And a similar work has also been performed in the driven elastic string in a disordered medium [32]. To our surprise, the difference of the roughness exponent ζ between these two models are neglectable within the errors, different from that at the depinning transition. And the overhangs vanish in the background with the finite velocity, which can be observed in Fig. 1(a). Hence, we can believe that overhangs lead to the main difference between this spin model and QEW. And $\zeta = 0.5$ is expected, for the quenched disorder acts effectively as a thermal noise at the largest scale with $\zeta_{therm} = 1/2$ [34, 35, 61].

Then in the driven RFIM, the transition point H_c and critical exponents β, ν, z, ζ can also be measured in the steady state with finite-size scaling and finite-temperature scaling forms. Based on the short-time dynamics scaling form, it is more convenient and precise for the determination of both dynamic and static exponents as well as transition point. Since one does not suffer from critical slowing down. For instance, the transition point H_c is reported

as 1.290(5) in Ref. [28]. While this curve with $H = 1.290$ visibly departure from the power law behavior, shown in Fig. 1(b). It means that the transition point H_c is distinctly above 1.290. What's more, in this work, we can investigate the roughness behavior carefully and systematically at the depinning transition. While for the RFIM in the steady state, it is too hard to measure the roughness exponent ζ and dynamic exponent z . And in Table.I, these exponents with + are obtained in the critical avalanches process, instead of depinning transition. Then the critical exponents of the depinning transition is also obtained for the discrete dislocation dynamics, which are quite agree with the result of our work.

Experimental investigation of domain wall motion in magnetic systems takes place at finite temperatures. With the thermal activation, the sharp depinning transition is clearly rounded. In the creep regime with $H \ll H_c, T > 0$, the interface velocity does not vanish and the scaling behavior has been investigated [34, 43, 61]. And the local roughness exponent has been measured experimentally, shown in Tab. II. It is a litter larger than $\zeta_{eq} = 2/3$, obtained in the equilibrium state with $H = 0, T > 0$. Then in Refs.[27, 28, 35], influence of temperature on the depinning transition of driven interfaces has also been shown with $H = H_c, T > 0$ and the roughness exponent $\zeta = 1.25$ is obtained, the same as the one at the depinning transition [35]. And in the Ref.[34], $\zeta = 1.26(1)$ can also be obtained, even at the driving field H well below H_c . While in these experiment, H is not so small. Especially in Ref.[54], $H = 17.7kA/m$ is used, quite near the critical field $H_c \approx 40kA/m$. And these experimental result of the local roughness exponent are close to $\zeta_{loc} = 0.735(5)$, measured in our work. Hence, a crossover takes place from the equilibrium state to the depinning states, as the driving filed is increased [34]. And in Ref.[61], a similar crossover has been investigated as the temperature is decreased.

IV. CONCLUSION

In summary, with Monte Carlo simulation we have investigated the non-equilibrium critical dynamics of the two-dimensional driven random-field Ising model for the depining transition and its background at zero temperature. The dynamic scaling behavior is carefully analyzed, and a dynamic roughening process is observed. The transition point and critical exponents are totally listed in Table I. Based on the short-time dynamics, it is more convenient and precise to measure these exponents than the work in the steady state close to the

depinning transition. The conjecture that the motion of a domain wall in a random-field system can be described by the equation EW with quenched disorder is in doubt here. And intrinsic anomalous scaling and spatial multiscaling are observed in the interface growth process of our work, quite different from the superrough scaling and spatial single scaling in QEW. When the overhangs vanish with the large driving field, the difference between these two models disappears. Hence, we conjecture that overhangs lead to the main difference between QEW and RFIM at the depinning transition. What's more, the local roughness obtained in this work is supported by the results of experiment, shown in Tab.II. But the effect of overhangs should be studied further. And it is also important to investigate the short-time dynamic behavior at lower temperature in RFIM and/or the transition between the relaxation, creep, slide, and switch regions with an oscillating driving field $H = H_0 \exp(i\omega t)$. Finally, the techniques used in this paper can be also applied to similar dynamic systems, such as xy model.

Acknowledgements: This work was supported in part by NNSF (China) under grant No. 10875102.

-
- [1] H.K. Janssen, B. Schaub, and B. Schmittmann, Z. Phys. **B73**, 539 (1989).
 - [2] H.J. Luo, L. Schülke, and B. Zheng, Phys. Rev. Lett. **81**, 180 (1998).
 - [3] B. Zheng, Int. J. Mod. Phys. **B12**, 1419 (1998), review article.
 - [4] B. Zheng, M. Schulz, and S. Trimper, Phys. Rev. Lett. **82**, 1891 (1999).
 - [5] Z.B. Li, L. Schülke, and B. Zheng, Phys. Rev. Lett. **74**, 3396 (1995).
 - [6] B. Zheng, F. Ren, and H. Ren, Phys. Rev. **E68**, 046120 (2003).
 - [7] J.Q. Yin, B. Zheng, and S. Trimper, Phys. Rev. **E70**, 056134 (2004).
 - [8] J.Q. Yin, B. Zheng, and S. Trimper, Phys. Rev. **E72**, 036122 (2005).
 - [9] N.J. Zhou and B. Zheng, Europhys. Lett. **78**, 56001 (2007).
 - [10] N.J. Zhou and B. Zheng, Phys. Rev. **E77**, 051104 (2008).
 - [11] X.W. Lei and B. Zheng, Phys. Rev. **E75**, 040104 (2007).
 - [12] L. Schülke and B. Zheng, Phys. Rev. **E62**, 7482 (2000).
 - [13] S.Z. Lin and B. Zheng, Phys. Rev. **E78**, 011127 (2008).
 - [14] S.G. Lemay, R.E. Thorne, Y. Li and J.D. Brock, Phys. Rev. Lett. **83**, 2793 (1999).

- [15] D.T. Fuchs, E. Zeldov, T. Tamegai, S. Ooi, M. Rappaport, and H. Shtrikman, Phys. Rev. Lett. **80**, 4971 (1998).
- [16] A. Dourlat, V. Jeudy, A. Lemaître, and C. Gourdon, Phys. Rev. **B78**, 161303(R) (2008).
- [17] M. Yamanouchi, J. Ieda, F. Matsukura, S.E. Barnes, S. Maekawa, and H. Ohno, Science **317**, 1726 (2007).
- [18] T. Tybell, P. Paruch, T. Giamarchi, and J.-M. Triscone, Phys. Rev. Lett. **89**, 097601 (2002).
- [19] P. Paruch, T. Giamarchi, and J.-M. Triscone, Phys. Rev. Lett. **94**, 197601 (2005).
- [20] S. Moulinet, A. Rosso, W. Krauth, and E. Rolley, Phys. Rev. **E69**, 035103(R) (2004).
- [21] P.L. Doussal, K.J. Wiese, E. Raphael, and R. Golestanian, Phys. Rev. Lett. **96**, 015702 (2006).
- [22] S.J. He, G.L.M.K.S. Kahanda, and P.Z. Wong, Phys. Rev. Lett. **69**, 3731 (1992).
- [23] S. Zapperi and M. Zaiser, Mater. Sci. Eng. **A309**, 348 (2001).
- [24] B. Bakó, D. Weygand, M. Samaras, W. Hoffelner, and M. Zaiser, Phys. Rev. **B78**, 144104 (2008).
- [25] L. Ponson, D. Bonamy, and E. Bouchaud, Phys. Rev. Lett. **96**, 035506 (2006).
- [26] L. Roters, A. Hucht, S. Lübeck, U. Nowak, and K.D. Usadel, Phys. Rev. **E60**, 5202 (1999).
- [27] L. Roters, S. Lübeck, and K.D. Usadel, Phys. Rev. **E63**, 026113 (2001).
- [28] U. Nowak and K.D. Usadel, Europhys. Lett. **44**, 634 (1998).
- [29] P.L. Doussal, K.J. Wiese, and P. Chauve, Phys. Rev. **B66**, 174201 (2002).
- [30] M. Jost and K.D. Usadel, Phys. Rev. **B54**, 9314 (1996).
- [31] M. Jost and K.D. Usadel, in *Chaos and Fractals in Chemical Engineering*, edited by G. Biardi, M. Giona, and A.R. Giona (World Scientific, Singapore, 1997).
- [32] O. Duemmer and W. Krauth, Phys. Rev. **E71**, 061601 (2005).
- [33] A.B. Kolton, A. Rosso, E.V. Albano, and T. Giamarchi, Phys. Rev. **B74**, 140201(R) (2006).
- [34] A.B. Kolton, A. Rosso, T. Giamarchi, and W. Krauth, Phys. Rev. Lett. **97**, 057001 (2006).
- [35] S. Bustingorry, A.B. Kolton, and T. Giamarchi, Europhys. Lett. **81**, 26005 (2008).
- [36] T. Nattermann, S. Stepanow, L.H. Tang, and H. Leschhorn, J. Phys. II France **2**, 1483 (1992).
- [37] H. J. Jensen, J. Phys. A: Math. Gen. **28**, 1861 (1995).
- [38] H. Leschhorn and L.H. Tang, Phys. Rev. Lett. **70**, 2973 (1993).
- [39] L.H. Tang, J. Stat. Phys. **67**, 819 (1992).
- [40] A. Rosso and W. Krauth, Phys. Rev. Lett. **87**, 187002 (2001).
- [41] A. Rosso, A.K. Hartmann, and W. Krauth, Phys. Rev. **E67**, 021602 (2003).

- [42] T. Goodman and S. Teitel, Phys. Rev. **E69**, 062105 (2004).
- [43] P. Chauve, T. Giamarchi, and P.L. Doussal, Phys. Rev. **B62**, 6241 (2000).
- [44] N.N. Pang and W.J. Tzeng, Phys. Rev. **E61**, 3559 (2000).
- [45] N.N. Pang and W.J. Tzeng, Phys. Rev. **E61**, 3212 (2000).
- [46] M. Pradas, A.H. Machado, and M.A. Rodríguez, Phys. Rev. **E77**, 056305 (2008).
- [47] M.A. Auger, L. Vázquez, R. Cuerno, M. Castro, M. Jergel, and O. Sánchez, Phys. Rev. **B73**, 045436 (2006).
- [48] M. Saitou, Phys. Rev. **B66**, 073416 (2002).
- [49] M. Saitou, K. Hamaguchi, and W. Oshikawa, J. Electrochem. Soc. **150**, C99 (2003).
- [50] S. Lemerle, J. Ferré, C. Chappert, V. Mathet, T. Giamarchi, and P.L. Doussal, Phys. Rev. Lett. **80**, 849 (1998).
- [51] P.J. Metaxas, J.P. Jamet, A. Mougin, M. Cormier, J. Ferré, V. Baltz, B. Rodmacq, B. Dieny, and R.L. Stamps, Phys. Rev. Lett. **99**, 217208 (2007).
- [52] W. Kleemann, J. Rhensius, O. Petravic, J. Ferré, J.P. Jamet, and H. Bernas, Phys. Rev. Lett. **99**, 097203 (2007).
- [53] T. Braun, W. Kleemann, J. Dec, and P.A. Thomas, Phys. Rev. Lett. **94**, 117601 (2005).
- [54] M. Jost, J. Heimel and T. Kleinefeld, Phys. Rev. **B57**, 5316 (1998).
- [55] T. Nattermann, V. Pokrovsky, and V.M. Vinokur, Phys. Rev. Lett. **87**, 197005 (2001).
- [56] A. Glatz, T. Nattermann, and V. Pokrovsky, Phys. Rev. Lett. **90**, 047201 (2003).
- [57] R. Bruinsma and G. Aeppli, Phys. Rev. Lett. **52**, 1547 (1984).
- [58] G.P. Zheng and M. Li, Phys. Rev. **E63**, 036122 (2001).
- [59] E.T. Seppälä, V. Petäjä, and M.J. Alava, Phys. Rev. **E58**, R5217 (1998).
- [60] G.R. Rodríguez, A.P. Junquera, M. Vélez, J.V. Anguita, J.I. Martín, H. Rubio, and J.M. Alameda, J. Phys. D: Appl. Phys. **40**, 3051 (2007).
- [61] A.B. Kolton, A. Rosso, and T. Giamarchi, Phys. Rev. Lett. **94**, 047002 (2005).
- [62] C.S. Nolle, B. Koiller, N. Martys, and M.O. Robbins, Physica **A205**, 342 (1994).
- [63] L.A.N Amaral, A.L Barabási, and H.E. Stanley, Phys. Rev. Lett. **73**, 62 (1994).
- [64] J.M. López and M.A. Rodríguez, J. Phys. I France **7**, 1191 (1997).

Exponent		QEW	RFIM	Dislocation	This work
$v(t)$	H_c		1.290(5)[28]		1.2933(2)
	β	0.33[33];0.33(2)[32]	0.35(4)[28];0.42(5)[62];0.31(8)[63]	0.30(5)[24]	0.295(2)
	ν	1.33[33];1.29(5)[32]	1.00(5)[28];1.33[62]	1.05(5)[24]	1.02(1)
	z	1.5[33];1.54(5)[29]		1.32(4)[24]	1.33(1)
$\omega^2(t)$	ζ	1.25[33];1.26(1)[32]			1.14(1)
$C(r, t)$	ζ	1.2[64];1.23(1)[45]		0.98(3)[24]	1.13(1)
	ζ_{loc}	0.92[64];0.98[31]		0.96(2)[24]	0.735(5)
<hr/>					
$H \gg H_c$	z_b	1.5[33]			1.50(1)
	ζ_b	0.5[32]	0.5[62]		0.487(5)

TABLE I: Summary of critical exponents are shown for the depinning transition (upper sector) and its background(lower sector), obtained with different techniques. Second column: result of numerical simulation obtained for the driven Edwards-Wilkinson equation with quenched disorder (QEW). Third column: result of numerical simulation obtained for the driven random field Ising model (RFIM) close to the transition point in the steady state. Forth column: result of numerical simulation obtained for the discrete dislocation model at the depinning transition. Then our work is shown in the last column, and the result of numerical simulation is obtained for the random field Ising model at the depinning transition with the short-time critical dynamic.

	This work	Ref.[50]	Ref.[54]	Ref.[51]	Ref.[52]
ζ_{loc}	0.735(5)	0.69(7)	0.78(1)	0.7(1)	0.6(1)

TABLE II: The local roughness exponent for the depinning transition in our work is shown here. In comparison, the result of experimental investigation of domain wall motion in magnetic systems are also listed in its creep regime. Refs.[50–52] work in the ultrathin Pt/Co/Pt films and Ref.[54] works in Co₂₈Pt₇₂ alloy films. And an oscillating driving field $H(t)$ is used in Ref.[52], instead of a dc driving field.

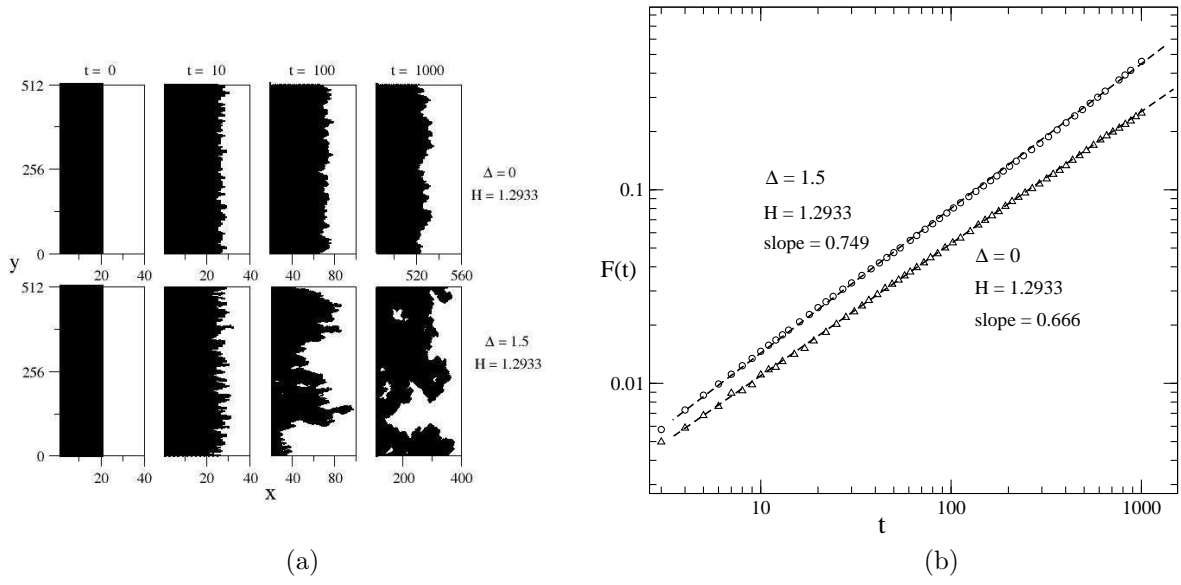


FIG. 1: (a) The time evolution of the interface velocity $v(t)$ is displayed for different driving field H when the disorder is fixed as $\Delta = 1.5$. For clarity, the curve with depinning field $H_c = 1.2933$ is shifted down by a factor 0.5. Dashed line shows the power law fit. Open squares corresponds to the different lattice size with $L = 1024$. (b) The function $F(t)$ is displayed with open dots on a log-log scale for the depinning transition (above) and its background (below). And dashed lines show the power law fits.

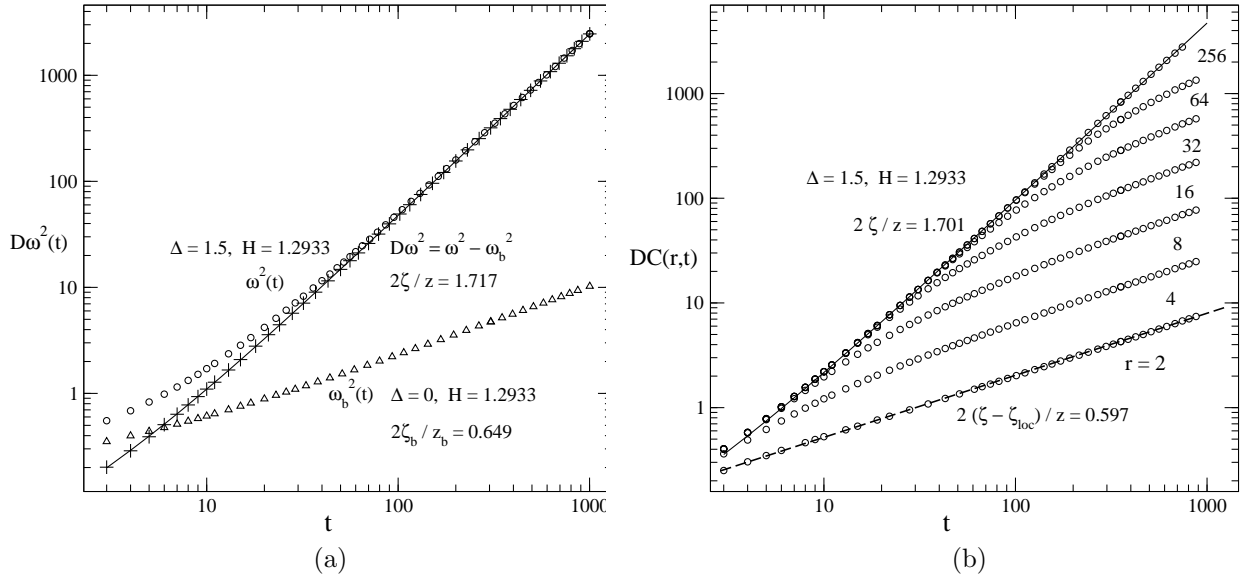


FIG. 2: (a) The roughness function $\omega^2(t)$ is plotted on a double-log scale with open dots. And pluses represent the pure roughness function $D\omega^2(t)$. Solid lines represent power law fits with correction, basing on Eq. 17. (b) The pure height correlation function $DC(r, t)$ is plotted with open circles on a log-log scale, for $r = 2, 4, 8, 16, 32, 64$ and 256 (from below). Dashed lines show the power law fits, and solid line represents a power law fit with correction. In the inset, $DC(r, \infty)$ vs. r is plotted for the depinning transition at its maximum time $t = 1024$. Data are fitted with solid lines, according to Eq. 15.